

Liquid-Phase Nanolithography in Hexadecane

Undergraduate Researcher
Matthew J. Schmitz, Northwestern University

Faculty Mentor
Mark Hersam
Department of Materials Science and Engineering,
Northwestern University

Graduate Student Mentor
C. Reagan Kinser
Department of Materials Science and Engineering,
Northwestern University

Abstract

In this study liquid-phase nanolithography (LPN) techniques using conductive atomic force microscopy are investigated in order to study properties of nano-patterned organic molecules covalently bound to a silicon substrate. Previous work has shown that LPN in the inert organic solvent hexadecane forms patterned features on hydrogen-passivated Si(111). Due to hexadecane's inert nature, it is believed that the features are formed by field-induced oxidation of the silicon substrate rather than by patterning hexadecane molecules on the surface. To investigate this hypothesis, the effects of lithographic parameters in the hexadecane system are compared with those in published data on field-induced oxidation of hydrogen-passivated silicon. Due to the number of reports analyzing line- and dot-patterned field-induced oxides, similar geometries of LPN features are also considered in this study. Initial analysis of LPN line patterns formed in hexadecane shows that these features are in fact due to field-induced oxidation. However, to increase the accuracy and validity of such findings, additional experiments and analysis are under way. Such findings will enable control and optimization of future experiments of patterning organic solute molecules in hexadecane on silicon via LPN.

Introduction

Liquid-phase nanolithography is a technique for patterning organic molecules directly on hydrogen-terminated silicon surfaces using conductive atomic force microscopy (AFM) in a liquid environment.¹ In recent work it has been observed that the silicon surface is modified under LPN patterning conditions in hexadecane, an inert organic solvent. Due to its inert nature, hexadecane should not react with the surface upon patterning. This study aims to characterize the features formed in hexadecane and to compare their growth kinetics to field-induced oxidation (FIO) growth kinetics as reported in literature. In FIO a sample bias is applied between a conductive AFM tip and the silicon substrate in air. The water meniscus that forms at the tip-sample

junction acts as a nano-electrochemical cell, resulting in localized silicon surface oxidation. Analysis of growth kinetics is accomplished by investigation of the effects of varying lithographic parameters, i.e., write speed, sample bias, and ambient humidity.

Background

Studies involving growth of organic monolayers on silicon surfaces have been motivated by integration of these systems into semiconductor technology²⁻⁴ In order to reduce the size of these systems to the nanometer length scale for integration with future microelectronics, LPN with a conductive atomic force microscope has been developed. To date, most research involving nanometer-sized modification

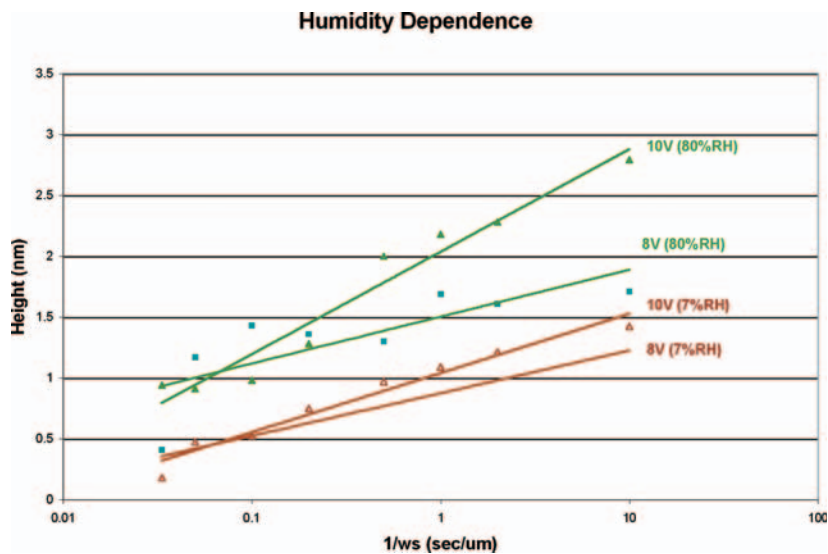


Figure 1: LPN data for line experiments run in hexadecane. Feature heights increase with relative humidity and logarithmically increase with time. (Linear fits are basic logarithmic fits to aid in viewing the data.)

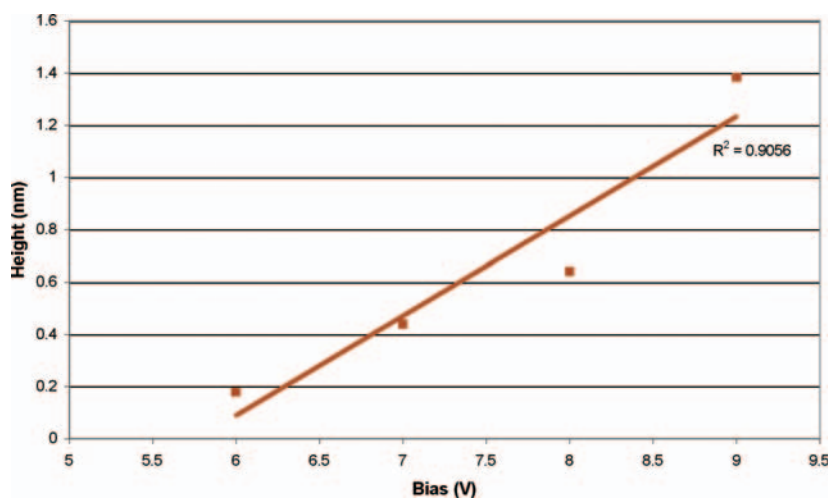


Figure 2: An example of linear feature height dependence on applied bias. Write speed is 1 $\mu\text{m/s}$, and RH is 7 percent.

of hydrogen-passivated silicon substrates with a conductive probe AFM has involved localized surface oxidation by applying a voltage bias between the cantilever tip and substrate.⁵⁻⁷ Additional work has shown evidence for patterning of conjugated alkynes directly to hydrogen-passivated silicon via scanning probe-induced cathodic electrografting.⁸ More recently, studies of LPN patterns made in neat undecylenic acid methyl ester (UDAME) give evidence of UDAME monolayer patterning.¹ This project furthers such lithography techniques by analyzing intrinsic patterning characteristics of LPN in hexadecane in an effort to evaluate its potential as a carrier medium for various patterning molecules.

Due to the amount of research that has been done on the kinetics of FIO with conductive AFMs, lithography patterns can be characterized by comparing their growth kinetics to that of field-induced

oxides. Avouris et al showed increased patterned feature height for an increase from 14 to 61 percent relative humidity (RH),⁶ along with an exponential relationship between oxide growth rate and the present oxide height.

$$b(t, V) = \frac{V}{E_0} \ln \left[R \frac{E_0}{V} t + 1 \right] \quad (1)$$

In 2000, Snow et al reported Equation (1) as an integration of the Avouris rate equation and a fit to scanned probe oxidation on hydrogen-passivated silicon.⁵ In this equation height is roughly linearly dependent on the applied bias and logarithmically dependent on the time of applied bias. E_0 and R are fitting parameters where R is the maximum oxidation rate and depends on the concentration of water molecules at the tip-sample junction. Upon comparing oxidation of hydrophobic and hydrophilic silicon surfaces, they note a 10^4 increase in R values.

Approach

This project's work of analyzing feature growth kinetics began with patterning sets of lines while varying experimental parameters and moved on to patterning dots with similar variation of parameters. Both line and dot patterns were analyzed due to their potential difference in growth kinetics.

The kinetic growth comparison for this project thus primarily involved fitting Equation (1) to height data from LPN line and dot features patterned in hexadecane while varying write speed or dwell time, applied bias, and RH. (Relative humidity in this case relates to the humidity at which the tip was held for one hour before immersion in hexadecane, in addition to the ambient humidity surrounding the system during patterning.) In the case that the patterns formed in hexadecane are oxides, they should follow increasing growth behavior similar to FIO, and not increasing then static behavior as seen with UDAME. In addition to similar growth behavior, comparison of fit E_0 and R values would give evidence as to whether or not FIO patterns are formed.

Silicon samples were sectioned from n-type Si(111) wafers. They were then passivated by 15-second immersion in a 0.5 percent HF solution, 10-minute immersion in a piranha solution (70 percent H_2SO_4 + 30 percent H_2O_2), and 15-minute immersion in an argon sparged 40 percent NH_4F solution. The samples were immersed in Ar sparged deionized water between each step. LPN was performed with a Thermomicroscopes CP Research scanning probe microscope using p++-type Si Ultralevers and a Thermomicroscopes MicroCell. Patterning experiments were run between 7 and

80 percent RH and at 26° C. Measurements of patterned feature dimensions were taken from intermittent contact mode AFM images after lithography and cleaning of the sample. Commercial software allowed for collection of height values for each line, taking the average maximum height along the length of the line. A home-built software program is used for collecting the maximum height and full width at half maximum (FWHM) for each patterned dot.

Results and Discussion

The applied bias ranged from 2 to 10 V, while patterning occurred at 6 V or greater. As seen in Figures 1 and 2, initial analysis of height data from hexadecane LPN line features shows logarithmic dependence on time (inverse write speed) and linear dependence on applied bias. Additionally, Figure 1 shows an increase in feature height with increased humidity. As presumed, humidity did have an effect on feature heights and widths, presumably due to an increase in the concentration of water molecules at the tip-sample junction.

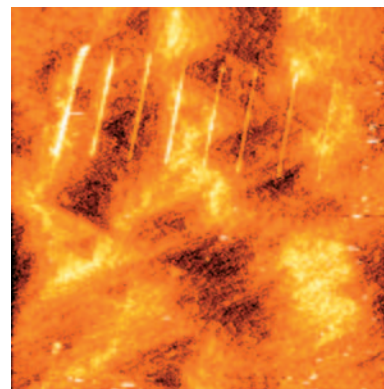
Due to the fact that inverse write speed was used as the time parameter, the equation fit to the data was

$$b(t, V) = \frac{V}{E_0} \ln \left[R d \frac{E_0}{V} (ws)^{-1} + 1 \right] \quad (2)$$

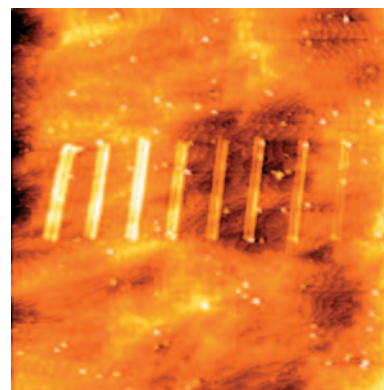
In this case d is an effective patterning length on the order of 10 nm that, when multiplied by inverse write speed, gives an appropriate time value. The constants used in fitting then become $1/E_0$ and RdE_0 . Using the Marquardt-Levenburg least squares method for fitting all of the data resulted in poor-fitting constants for describing the experimental data. Since line features showed single- and

double-tip effects as seen in Figure 3 a and b, it was determined that the tip conditions could be inconsistent between patterning experiments. Most of the data showed consistent height behavior within a single experiment, but some of the data showed slight variation in the behavior between experiments. Table 1 gives the fitting constants for groupings of experiments showing minimal variation between each. Fitted E_0 values are relatively close to 45 V/nm as listed by Snow. Fitted RdE_0 values on average are on the order of 10^3 . With estimated d values ranging from 50 to 100 nm depending on the line width, corresponding R values are on the order of 0.1 to 1 nm/s, which is significantly lower than ambient values of 10^3 to 10^7 reported by Snow. These lower R values are expected due to the dependence of R on concentration of water molecules and the hydrophobic nature of hexadecane. Figure 4 shows the data and fit lines for LPN experiments run at 80 percent RH. A fair amount of scatter between the data points and their corresponding fits exists, in addition to nonlinear spacing of each fit line for a given write speed. Figure 5 shows the data for the same experiments run at 7 percent RH. In these experiments enough data points did not exist at lower bias, so fits to Equation 2 were done for 8 and 10 V data. This experiment yielded less scatter in the data than the higher humidity case.

Running further experiments with better tip conditions would increase the size and accuracy of the data set. In addition, this could allow for analysis of additional effects that were not originally accounted for, such as a height dependence on cantilever tip patterning history, the possibility of running out of the water or oxygen source with subsequent patterning, and the potential for any meniscus



a.



b.

Figure 3: Representative AFM topography images showing the difference in experiments with single- and double-tip effects. Images were taken in intermittent contact mode.

- a) 5 μm image with single-tip effect.
- b) 4.5 μm image with double-tip effect.

Liquid-Phase Nanolithography in Hexadecane (*continued*)

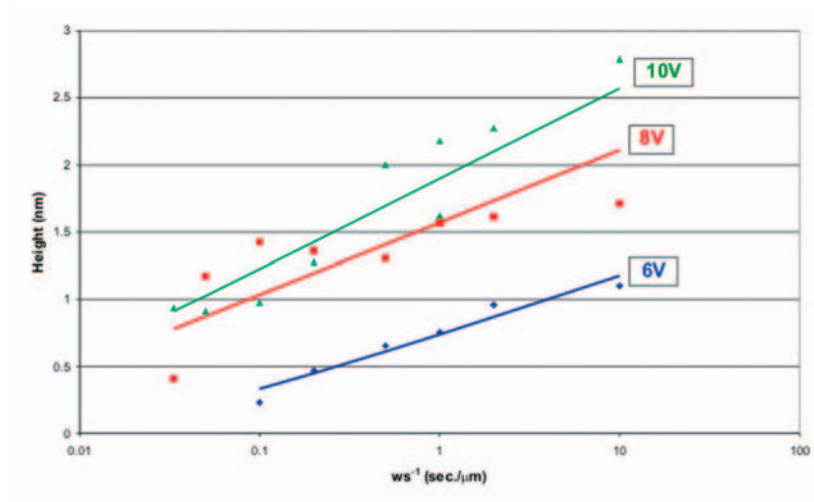


Figure 4: Height data for experiments run at 80 percent RH. Linear fits are based on Equation 2. Noticeable scatter is seen for 8 and 10 V data.

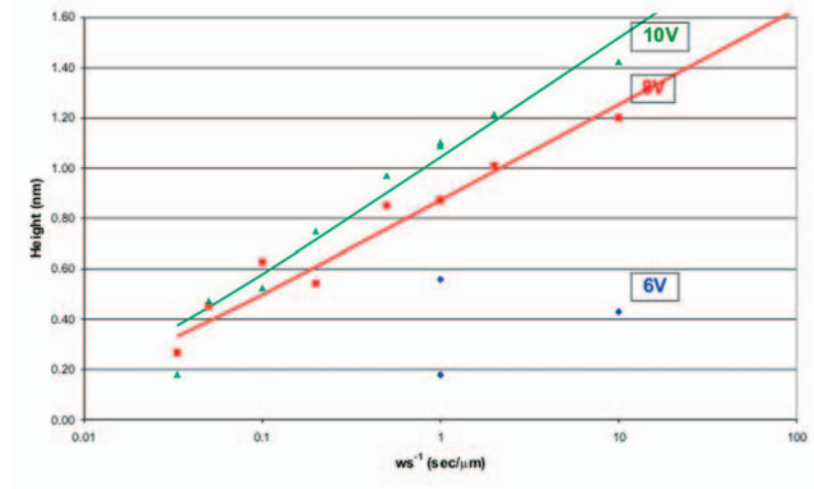


Figure 5: Height data for experiments run at 7 percent RH. Linear fits are based on Equation 2. Less scatter is seen for 8 and 10 V data.

Table 1: Fitting parameters from Equation 2 on grouped data sets.

Group	E_0 (V/nm)	Rd E_0 ($\mu\text{m/s}$)
8 and 10 V (7% RH)	48	1533
8 and 10 V (80% RH)	34	6399
6 V (80% RH)	31	283

formation effects in hexadecane similar to those reported by Snow for ambient FIO. Lastly, analysis of the same LPN experiments run in air to create FIO patterns would allow for reproduction of Snow's data in addition to providing a baseline comparison specific to this project's LPN data.

To date, LPN experiments forming dot patterns under varying lithographic parameters similar to those for the line patterns are in the process of being completed and analyzed.

Conclusions

LPN line patterns formed in hexadecane are consistent with field-induced oxides. The growth kinetics of the LPN patterned features exhibit the expected linear dependence on applied bias and logarithmic dependence on time. Furthermore, the size of the patterned features increases with increasing humidity. Similar experiments in other polar solvents would allow for analysis of patterning dependence on dielectric behavior of the solvent. With such information one could then work toward finding optimal organic solute-solvent solutions for LPN of various desired patterning molecules.

References

- (1) Baluch, A. S.; Basu, R.; Guisinger, N. P., et al. *Mat. Res. Soc. Symp. Proc.* **2003**, *750*, Y9.1.1
- (2) Linford, M. R.; Fenter, P.; Eisenberger, P. M., et al. *J. Am. Chem. Soc.* **1995**, *117*, 3145–3155.
- (3) Wagner, P.; Nock, S.; Spudich, J. A., et al. *J. Struct. Biol.* **1997**, *119*, 189–201.
- (4) Zhao, J.; Uosaki, K. *Appl. Phys. Lett.* **2003**, *83*, 2034–2036.
- (5) Snow, E. S.; Jernigan, G. G.; Campbell, P. M. *Appl. Phys. Lett.* **2000**, *76*, 1782–1784.
- (6) Avouris, P.; Hertel, T.; Martel, R. *Appl. Phys. Lett.* **1997**, *71*, 285–287.
- (7) Stiévenard, D.; Fontaine, P. A.; Dubois, E. *Appl. Phys. Lett.* **1997**, *70*, 3272–3274.
- (8) Hurley, P. T.; Ribbe, A. E.; Buriak, J. M. *J. Am. Chem. Soc.* **2003**, *125*, 11334–11339.